

Journal of Biomedical Optics

SPIEDigitalLibrary.org/jbo

Addressable multiregional and multifocal multiphoton microscopy based on a spatial light modulator

Yonghong Shao
Wan Qin
Honghai Liu
Junle Qu
Xiang Peng
Hanben Niu
Bruce Z. Gao

Addressable multiregional and multifocal multiphoton microscopy based on a spatial light modulator

Yonghong Shao,^a Wan Qin,^b Honghai Liu,^b Junle Qu,^a Xiang Peng,^a Hanben Niu,^a and Bruce Z. Gao^b

^aShenzhen University, College of Optoelectronics Engineering, Key Laboratory of Optoelectronic Devices and Systems of Ministry of Education and Guangdong Province, Shenzhen 518060, China

^bClemson University, Department of Bioengineering and COMSET, Clemson, South Carolina 29634

Abstract. Through a combination of a deflective phase-only diffractive spatial light modulator (SLM) and galvo scanners, an addressable multiregional and multifocal multiphoton microscope (AM-MMM) is developed. The SLM shapes an incoming mode-locked, near-infrared Ti:sapphire laser beam into multiple beamlet arrays with addressable shapes and sizes that match the regions of interest on the sample. Compared with conventional multifocal multiphoton microscope (MMM), AM-MMM achieves the effective use of the laser power with an increase of imaging rate and a decrease of photodamage without sacrifice of resolution.

© 2012 Society of Photo-Optical Instrumentation Engineers (SPIE). [DOI: 10.1117/1.JBO.17.3.030505]

Keywords: multiphoton microscopy; multifocus; spatial light modulator; addressable scanning; dynamic imaging.

Paper 11665L received Nov. 10, 2011; revised manuscript received Dec. 28, 2011; accepted for publication Jan. 4, 2012; published online Apr. 3, 2012.

1 Introduction

In biomedical research, multiphoton microscopy is a powerful tool capable of deep penetration into strongly scattering specimens and 3D imaging of living cells at high resolution without use of confocal aperture.^{1,2} Multiphoton fluorescence can be generated only at very high peak intensity, which can be achieved by focusing a femtosecond (fs) laser beam to its diffraction limit; such intensity cannot be achieved by illuminating the full field, even with laser power that approaches the photodamage threshold. In addition, the power required to generate the peak intensity is relatively low and cannot be so high as to cause photodamage. Thus, in conventional multiphoton microscopy, only a very small portion of the laser power is useful, and point-by-point scanning of the entire field of view (FOV) gives a very low imaging rate. To make full use of the laser's power and simultaneously increase the imaging rate, multifocal multiphoton microscopy (MMM) has been developed: The laser's full power is distributed into multiple beamlets that are focused to form a multifocal array. At each focal point, multiphoton fluorescence is generated with appropriate peak power and without photodamage. Each

beamlet is required to scan only a subregion, and the entire FOV is scanned in parallel by the multifocal array so that the effective acquisition rate is approximately equal to the original single-beam rate multiplied by the number of beamlets.

Initially, MMM utilized microlenses or cascaded beamsplitter arrays to generate the multifocal array,^{3,4} and the scanning was achieved using galvo scanners. Recently, a spinning disk with microlenses has been used to construct an MMM; it achieved an imaging rate of up to 1000 frames per second (fps).³ However, with the combination of microlenses and galvo mirrors, there is a loss of incident power of nearly 75%.⁵ Using the spinning disk with microlenses also causes an unavoidable loss of power from beam expansion and optical trains. In addition, the nonuniformity of probe intensity in these systems causes the peripheral regions of the image to be 50% less intense than the center.³ More recently, a miniature, low-cost diffractive optical element (DOE) in tandem with galvo scanners has been applied to produce an array of up to 10×10 focal points with a diffraction efficiency of 75% and uniformity in focal intensity within 1%.⁶ With this DOE system, an MMM that is 1000-fold faster than a conventional single-beam multiphoton microscope is achieved using stochastic scanning.⁷ When the entire FOV is scanned with an MMM, the imaging rate increases as the number of beamlets increase. However, with the increase of the number of beamlets, the power of each beamlet decreases, resulting in a low signal to noise ratio. Therefore total available power, which is determined by the laser and the damage threshold of the optics [e.g., the spatial light modulator (SLM)] used in the system, limits the number of beamlets and thus the image rate. In some applications, however, only a small area of the FOV contains the features that must be rapidly imaged with high resolution. For example, when studying a sarcomere's contraction, we first locate a target muscle cell in the FOV. We then focus the image system into this cell body to acquire high resolution images of the sarcomere at a very high rate that freezes the contraction. In such cases, a small number of beamlets can be used to scan the FOV with low speed and resolution and then scan the area(s) of interest selected rapidly with high resolution. A SLM can be used to realize this addressable multifocal imaging concept. Scanless microscopy has been developed using a SLM, which distributes the illumination light dynamically into multiple areas of interest.⁸ In scanless SLM microscopy, however, a lack of the confocal gate for 3D sectioning and multiphoton excitation occurs when an entire area of interest is simultaneously illuminated.

Here, we report the design of an addressable multiregional MMM (AM-MMM) that comprises of SLM and galvo scanners to produce multiple focal arrays. The SLM we used is based on reflective liquid crystal on silicon, which modulates an incident light beam spatially in phase to generate dynamic beamlets according to the displayed phase image that is transferred by a computer interface. By altering the phase image, the orientation of the beamlets can be changed, and thus multibeam scanning can be achieved. However, the transfer rate of the phase image for a commercially available SLM is too slow (less than 100 Hz) to achieve high-speed imaging. Consequently, we should use the SLM to achieve only beam splitting (without scanning), and use a pair of galvo scanners to realize image scanning. For this purpose, the SLM can be modeled as a DOE coupled with a reflecting mirror: The DOE feature will

Address all correspondence to: Bruce Z. Gao or Junle Qu, Clemson University, Department of Bioengineering and COMSET, Clemson, South Carolina 29634. Tel: (864) 656-3311; E-mail: zgao@clemson.edu or jlqu70@gmail.com.

allow the SLM to split the incident beam into multiple beamlets, and the mirror feature will permit the SLM to reflect the incident beam with various incident angles into the conjugated angle according to Snell's Law, thus achieving beam scanning. Consider a traveling plane wave: $E_{in} = \exp[i(kx \cos \alpha + ky \cos \beta)]$ at $z = 0$ plane, where E_{in} is the optical field, k is the wave vector, x and y are the coordinates in the x - y plane parallel to the SLM surface, $\cos \alpha$ and $\cos \beta$ are the direction cosines, α and β are functions of the incident angle θ (an angle between the incident wave and the SLM surface's normal). A phase-modulated function of the phase-only SLM can be expressed as: $E_{mod} = \exp[i\Phi(x, y)]$ in which Φ represents the phase-recovery function corresponding to the pattern of the focus array. Accordingly, the electronic field of the SLM-reflected wave can be expressed as: $E_{ref} = E_{in} \cdot E_{mod}$. The optical field at the focal plane of the Fourier lens will be given by:

$$G(u, v) = F(u, v) * \delta\left(u - \frac{\cos \alpha}{\lambda}, v - \frac{\cos \beta}{\lambda}\right) = F\left(u - \frac{\cos \alpha}{\lambda}, v - \frac{\cos \beta}{\lambda}\right), \quad (1)$$

where $F(u, v)$ is the Fourier transform of E_{mod} , $u = x/f\lambda$, $v = y/f\lambda$ and u and v are the coordinates on the Fourier plane. According to Eq. (1), when the incident angle changes, the focus array will be only translated in the (u, v) plane based on the relationship of $\Delta u = \cos \alpha/\lambda$ and $\Delta v = \cos \beta/\lambda$; the other features of the focus array, such as the shape and the number of foci, will not change. Especially when θ is very small, $\Delta u = \theta_{\parallel}/\lambda$ and $\Delta v = \theta_{\perp}/\lambda$, which means that the translation of the focus array is proportional to the change of the incidence angle. Therefore, a scanning focus array can be generated with a pair of galvo scanners by scanning the single beam (θ_{\parallel} in x direction and θ_{\perp} in y direction) that is incident to the SLM.

Multiple arrays of beamlets can be generated. The location and orientation of the beamlets and the beamlet number in each array are based on the location and shape of the corresponding area of interest to be illuminated. At the beginning of each imaging process, the entire FOV was scanned as in conventional MMM, with a focal array (e.g., 10×10) generated by the SLM. Using the image thus obtained, we selected the areas of interest and the numbers of arrays; the location, orientation, and inter-focal distance in each array were calculated using our lab's custom-designed software in MatLab. The image was then scanned regionally at high speed and with high resolution. An electron multiplying charge coupled device (EM-CCD) was used to record the two-photon fluorescence signals from different regions simultaneously. An AM-MMM so designed can (1) use the laser power effectively, (2) increase the imaging rate and resolution, and (3) decrease the risk of photodamage.

Figure 1 is a schematic of the AM-MMM composed of a phase-only SLM, galvo scanners, and our custom-built optical microscope consists of several Olympus microscopic components with an Olympus water-immersion objective (NA 1.0, 60 \times) and optical stages from ThorLabs.⁹ The laser beam from a mode-locked Ti:sapphire laser (Spectra-Physics, Tsunami pumped by a 10 W Millennia) is expanded and collimated to slightly overfill the phase-only SLM (Holoeye Pluto, near infrared (NIR), 1920 \times 1080 pixels, 8 bits), which is capable of completing 2π phase modulation at each pixel with a 60 Hz refresh rate. The SLM can be used to dynamically produce arbitrary

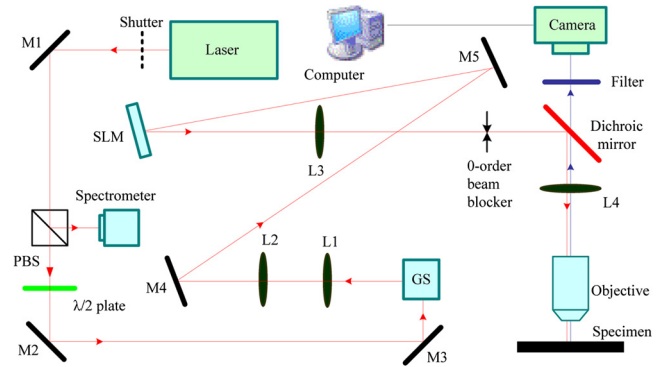


Fig. 1 Schematic of the AM-MMM based on the combination of an SLM and galvo scanners. The galvo scanners for the fs laser beam (GS) comprise x- and y-scanners on the front focal plane of a 4f system comprising L1 and L2. The SLM on the back focal plane of L2 modulates the input fs beam to generate multifocal arrays through a Fourier lens (L3) on the front focal plane of the tube lens (L4); the zero-order light is blocked by a blocker. The polarization of the fs beam is tuned by a $\lambda/2$ waveplate. Laser: a model-locked laser that generates an fs beam; M1 to 5: gold film mirrors; Camera: an EM-CCD.

patterns with computer-generated phase-only holograms. An accurate phase pattern can be generated by employing phase retrieval algorithms such as the classic Gerchberg-Saxton (GS) algorithm,¹⁰ or by directly utilizing the Holoeye application software. A Fourier lens with a focal length of 200 mm transfers the light that is phase-modulated by the SLM into an array of focal points at the back focal plane of the tube lens (the largest focal array is 15 mm, approximately the size of the microscope's FOV at that plane), the front focal plane of which is located at the entrance of the microscope objective. The objective then produces one or series of focus arrays at the sample plane. Because only the first order of diffraction is used, the unwanted zero order created by the SLM is blocked by a spatial filter. To achieve high resolution and sectioning capacity using the confocal gate according to wave optics calculations, the smallest interfocal distance is chosen to be approximately 6 μm .¹¹

The pattern of the addressable arrays is sequentially or stochastically scanned across a sample's multiple areas of interest by a two-mirror galvo scanner (Cambridge Tech) driven by a line-by-line or a normalized white-noise waveform generated by a NI-PCI6115 DAQ card. The fluorescence signal is separated from the NIR excitation light by a dichroic mirror (Semrock, FF665) and imaged by an Andor cooling CCD (DU-888E-C00-#DZ).

The flexibility and resolution of the AM-MMM was examined using a 760 nm laser beam with an average power of 2 mW for each beamlet. Figure 2(a) is a plot of the fluorescence-intensity profile along the center line of a 0.5 μm fluorescent bead. Figure 2(b) shows the distribution of the fluorescence intensity along z -axial in the beam center obtained by scanning the same 0.5- μm fluorescent bead. In terms of these data, the lateral and axial resolutions are estimated with a deconvolution procedure to be 0.46 and 1.26 μm .

Figure 3 shows a two-photon image of three adult cardiomyocytes, which are fluorescence-labeled for α -actinin, in three regions of the FOV. The phase pattern for generating the three focal arrays is produced based on the location and the shape of the three cells and then uploaded to the SLM. The pattern of the three arrays, which comprises 43 foci in total and is

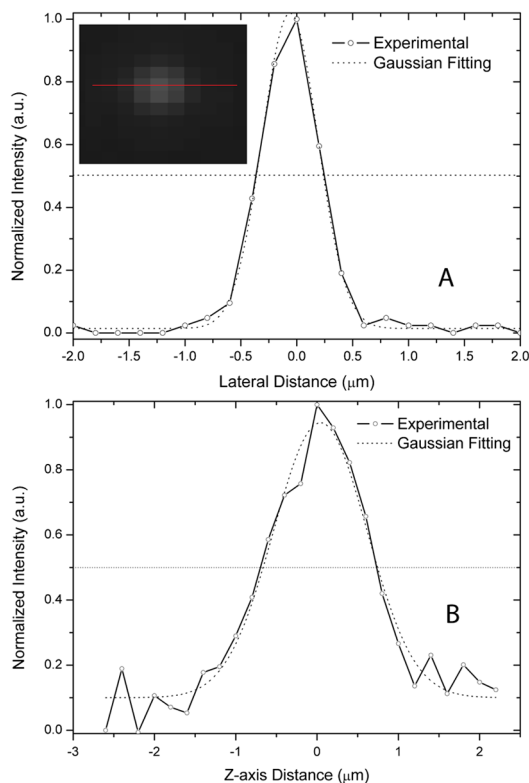


Fig. 2 The fluorescence-intensity profile along the center line obtained by scanning a $0.5 \mu\text{m}$ fluorescence bead along (a) the x-axis, where the lateral resolution is estimated to be $0.46 \mu\text{m}$, and (b) the z-axis, where the axial resolution is estimated to be $1.26 \mu\text{m}$.

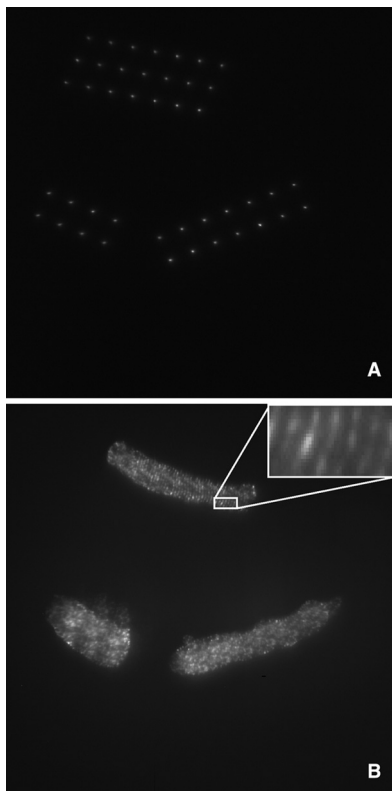


Fig. 3 (a) Pattern of three focal arrays that is generated with the full-field scanned coarse image of the three cells. (b) Image of the sarcomere structure in three adult cardiomyocytes stained for α -actinin, FOV = $200 \times 200 \mu\text{m}^2$.

produced by imaging a Rhodamine-6G film on coverglass, is shown in Fig. 3(a). The sarcomere structures are shown in Fig. 3(b). The laser power of 1 to 3 W from a typical fs laser can be used effectively in our MMM system. To rapidly image an FOV of $200 \times 200 \mu\text{m}^2$, we can use a dense foci array such as 30×30 with an interfocal distance of $6.5 \mu\text{m}$. The max power per focal point would be approximately 0.3 to 1 mW with the typical laser-to-focal-point delivery efficiency of 30%. This low power may not be sufficient for some applications such as imaging deep tissues. Using our MMM, we can increase power at the focal points by producing the desired foci pattern based on the imaging area of interest. For example, to image an adult cardiomyocyte in the FOV, we may use a focal array of 4×25 that is oriented along the cell axis. The laser power at each focal point can be adjusted to a typical value of 2 to 4 mW. By doing so, the laser power will be used effectively, and the temporal resolution will be high because a scan is unnecessary.

In conclusion, we have demonstrated an addressable AM-MMM, which can rapidly scan multiple regions in a sample according to the areas of interest. It improves the efficiency of use of the laser power while maintaining high spatial and temporal resolution and decreases photodamage to samples.

Acknowledgments

This work has been partially supported by NIH (SC COBRE P20RR021949 and Career Award 1k25hl088262-01), NSF (MRI CBET-0923311 and SC EPSCoR RII EPS-0903795 through SC GEAR program), The National Natural Science Foundation of China (31171372), Guangdong Province Science and Technology Project (10B060300002), Shenzhen University Application Technology Development Project (201136), and the Key Laboratory of Optoelectronic Devices and Systems of Ministry of Education and Guangdong Province (Shenzhen University).

References

1. V. E. Centonze and J. G. White, "Multiphoton excitation provides optical sections from deeper within scattering specimens than confocal imaging," *Biophys. J.* **75**(4), 2015–2024 (1998).
2. W. Denk, J. H. Strickler, and W. W. Webb, "2-Photon Laser Scanning Fluorescence Microscopy," *Science* **248**(4951), 73–76 (1990).
3. J. Bewersdorf, R. Pick, and S. W. Hell, "Multifocal multiphoton microscopy," *Opt. Lett.* **23**(9), 655–657 (1998).
4. D. N. Fittinghoff and J. A. Squier, "Time-decorrelated multifocal array for multiphoton microscopy and micromachining," *Opt. Lett.* **25**(16), 1213–1215 (2000).
5. A. H. Buist et al., "Real time two-photon absorption microscopy using multi point excitation," *J. Microsc.-Oxford* **192**(2), 217–226 (1998).
6. L. Sacconi et al., "Multiphoton multifocal microscopy exploiting a diffractive optical element," *Opt. Lett.* **28**(20), 1918–1920 (2003).
7. J. E. Jureller, H. Y. Kim, and N. F. Scherer, "Stochastic scanning multiphoton multifocal microscopy," *Opt. Express* **14**(8), 3406–3414 (2006).
8. V. Nikolenko et al., "SLM microscopy: scanless two-photon imaging and photostimulation with spatial light modulators," *Front. Neural Circ.* **2**, Article 5(1–14) (2008).
9. Y. Shao et al., "3D Myofibril Imaging in live cardiomyocytes via hybrid SHG-TPEF microscopy," *Proc. SPIE* **7903**, 79030F (2011).
10. J. M. Zaleskas et al., "Contractile forces generated by articular chondrocytes in collagen–glycosaminoglycan matrices," *Biomaterials* **25**(7–8), 1299–1308 (2004).
11. V. Andresen, A. Egner, and S. W. Hell, "Time-multiplexed multifocal multiphoton microscope," *Opt. Lett.* **26**(2), 75–77 (2001).